Redox Biology 14 (2018) 338–353

Contents lists available at ScienceDirect

Redox Biology

journal homepage: www.elsevier.com/locate/redox

Research Paper

Advanced oxidation protein products induce S-phase arrest of hepatocytes via the ROS-dependent, β-catenin-CDK2-mediated pathway

Shibo Sun[a,1], Fang Xie[b,1], Xiaoping Xu[b,1], Qing Cai[c], Qifan Zhang[a], Zhonglin Cui[a], Yujian Zheng[c], Jie Zhou[a,*]

[a] Department of Hepatobiliary Surgery, Nanfang Hospital, Southern Medical University, Guangzhou, Guangdong 510515, China
[b] Guangdong Provincial Key Laboratory of Gastroenterology, Department of Gastroenterology, Nanfang Hospital, Southern Medical University, Guangzhou, Guangdong 510515, China
[c] Department of Hepatobiliary Surgery and Liver Transplantation Center, Guangzhou General Hospital of Guangzhou Military Area, Guangzhou, Guangdong 510515, China

ARTICLE INFO

Keywords:
Advanced oxidation protein products
S-phase arrest
Reactive oxygen species
β-catenin
Cyclin-dependent kinase 2
Liver regeneration

ABSTRACT

Liver regeneration has important clinical importance in the setting of partial hepatectomy (PH). Following PH, quiescent hepatocytes can reenter cell cycle to restore liver mass. Hepatocyte cell cycle progression, as the basic motivations of liver regeneration, can be disrupted by multiple pathological factors such as oxidative stress. This study aimed to evaluate the role of advanced oxidation protein products (AOPP) in S-phase arrest in hepatocytes. Serum AOPP level were measured during the perioperative period of PH in 33 patients with hepatocellular carcinoma (HCC). Normal Sprague Dawley rats, human and murine liver cell line (HL-7702 and AML-12) were challenged with AOPP prepared by incubation of rat serum albumin (RSA) with hypochlorous acid, and the effect of AOPP on hepatocytes cell cycle progression and liver regeneration was studied after PH. AOPP levels were increased following partial hepatectomy (PH) in patients with primary liver cancer. AOPP treatment impaired liver regeneration in rats following 70% partial hepatectomy. S-phase arrest was induced by AOPP administration in hepatocytes derived from the remnant liver at controlled times following partial hepatectomy in rats, and in HL-7702 and AML-12 cells. The effect of AOPP on hepatocyte S phase arrest was mainly mediated by a nicotinamide adenine dinucleotide phosphate (NADPH) oxidase-dependent reactive oxygen species (ROS) generation, downregulation of downstream β-catenin signaling and decreased cyclin-dependent kinase 2 (CDK2) expression, which inhibited S-phase progression in hepatocytes. This study provides preliminary evidence that AOPP can induce S-phase arrest in hepatocytes via the ROS-dependent, β-catenin-CDK2-mediated pathway. These findings suggest a novel pathogenic role of AOPP contributing to the impaired liver regeneration and may provide the basis for developing new strategies to improve liver regeneration in patients undergoing PH.

1. Introduction

Partial hepatectomy (PH) is used in the treatment of patients with both malignant primary liver tumors and hepatic metastases [1]. Following PH, the remaining normal liver has a remarkable ability to regenerate via a process of compensatory hepatocellular proliferation [2,3]. Liver regeneration is dependent upon various pathways in regulation of the cell cycle [4,5]. Following PH, quiescent hepatocytes rapidly re-enter the cell cycle in a highly synchronized manner and undergo one or two rounds of cell division to proliferate and compensate for lost tissue [6,7]. Disruption of the hepatocyte cell cycle contributes to the impairment of liver regeneration and can result in liver failure [8,9].

Recently, oxidative stress has been shown to impair the cell cycle [10]. Advanced oxidation protein products (AOPP), is a newly described protein marker of oxidative stress that is generated under conditions of oxidative damage, and is recognized to be involved in oxidation-associated diseases [11], including chronic hepatitis and liver failure [12,13]. We have previously shown that AOPP is not only a marker for oxidative cell damage, but is also a novel class of pathogenic mediator via redox-dependent pathway [14]. Production of cytosolic Reactive oxygen species (ROS) can result from the activation of a series of enzymes, including NADPH oxidase, cyclooxygenase, nitric oxide synthase, with growing evidences that NADPH oxidase appears to be

* Correspondence author.
E-mail address: jacky_smu@163.com (J. Zhou).
[1] These authors contributed equally to this work.

http://dx.doi.org/10.1016/j.redox.2017.09.011
Received 11 September 2017; Accepted 18 September 2017
Available online 06 October 2017

the major cytosolic source of ROS generation in coronary artery disease and ischemic stroke [15,16]. Excessive ROS accumulation results in cell injury through oxidative stress and is involved in variety of human diseases, including diabetes, Crohn's disease and neurological disorders [17–21]. We have previously described that AOPP induced apoptosis of intestinal epithelial cells and intestinal injury via ROS generation [22]. In our previous *in vivo* and *in vitro* study, excessive intracellular ROS accumulation and hepatocyte S-phase arrest were observed following AOPP administration, which indicated that ROS may play a role in hepatocyte cell cycle regulation. Although a relationship between ROS and the cell cycle has previously been described [23,24], the exact mechanisms by which ROS regulates cell cycle progression in residual hepatocyte following PH have not been well explored.

Wnt/β-catenin is known to play a critical role in cells during oxidative stress, possibly in protective mechanisms [25,26]. β-catenin is the key factor of the Wnt/β-catenin signaling pathway; Wnt/β-catenin signaling is activated inside the cell mainly by the cellular redistribution and nuclear accumulation of the β-catenin gene [27,28]. Previous studies have shown that Wnt/β-catenin signaling takes part in hepatocytes proliferation by regulating cell cycle-related proteins, including cyclin D1 and c-myc [29,30]. For these reasons, there is increasing evidence to support the role of ROS in suppressing the activation of Wnt/β-catenin [13,31]. Therefore, we wished to determine the role of β-catenin as a possible 'bridge' between ROS and residual hepatocyte cell cycle arrest following PH, and to use a rat model and cultured cell models that we have previously established.

The aims of the present study were to investigate the effect of AOPP in liver regeneration following PH in a rat model *in vivo* and to evaluate the role of AOPP in hepatocyte cell cycle *in vivo* and *in vitro*.

2. Results

2.1. Serum advanced oxidation protein products (AOPP) was increased in patients following partial hepatectomy

A total of 33 hepatocellular carcinoma (HCC) patients met the inclusion criteria and underwent partial hepatectomy (PH) during the study period. Serum advanced oxidation protein products (AOPP) levels in all patients increased significantly after surgery as compared with pre-PH, peaked at day 1 (173.01 ± 54.84 μmol/L, $P < 0.01$) and followed by a gradual decrease at day 3–5 following PH (Fig. 1A). In addition, Levels of albumin (indicators of hepatic synthetic function), the main substrate in AOPP formation, significantly decreased in the postoperative stage (Fig. 1A). The serum level of ALT and AST (indicators of liver damage) were also analyzed and shown to be significantly increased following PH, compared to pre-PH (Fig. 1A). The fluctuating trend of AOPP positively correlated with ALT and AST and inversely correlated with ALB, suggesting that serum AOPP accumulation might involve in impairing the recovery of liver following PH.

2.2. Impaired liver regeneration in AOPP-challenged rats was improved by treatment with N-acetylcysteine (NAC)

In an attempt to examine the effects of AOPP in the process of liver regeneration, normal male Sprague-Dawley (SD) rats were studied following the removal of 70% of their liver mass, as described previously [4]. After the partial hepatectomy (PH) operation, rats were randomly assigned into four groups and received intravenous injections of phosphate buffered saline (PBS), rat serum albumin (RSA), or AOPP every day with or without ROS scavenger *N*-acetylcysteine (NAC) at controlled times. The concentrations of circulating ALT, AST and ALB were measured (Fig. 1B). Administration of AOPP significantly increased ALT, and AST levels and reduced the levels of ALB in a reactive oxygen species (ROS)-dependent manner (Fig. 1B).

Liver histology in the rat showed mild vacuolar degeneration in the control and RSA groups at day 1 following PH, whereas in the liver histology in the AOPP-treated group showed massive vacuolar degeneration, necrosis, and cytoplasmic swelling of most surviving hepatocytes from day 1 to day 7 following PH (Supplemental Fig. 1). The ongoing liver injury, reflected by vacuolar degeneration and necrosis in hepatocytes, was improved by administration of NAC.

Regeneration of the liver was evaluated by examining remnant liver volume and comparing its weight to body weight (liver/body ratio). Normally, the process of liver regeneration takes 5–7 days to make up for the mass of the removed liver lobes [2]. The volume of remaining liver in the AOPP group was significantly smaller when compared with the control or RSA groups at day 7 following PH ($P < 0.01$) (Fig. 2A). AOPP-treated rats significantly reduced liver/body ratios and the reduction of liver/body ratio was maintained even at day 7 following PH when compared with control rats or RSA-treated rats ($P < 0.01$) (Fig. 2B).

In order to explore the mechanism of compromised liver regeneration, we examined cell proliferation in regenerating livers in the four groups using immunohistochemistry staining for the cell proliferation marker, proliferating cell nuclear antigen (PCNA) (Fig. 2C). Normal adult rat liver exhibited less than 0.1% PCNA-positive cells. Remnant liver of control and RSA group rats displayed almost 100% of PCNA-positive hepatocytes at day 1 following PH. PCNA expression gradually declined in the later 6 days. Treatment of NAC improved remnant liver suffering from AOPP-induced recovery impairment of volume and liver/body ratio and reduced expression of PCNA. These results indicated that AOPP-ROS dependency impaired the liver regeneration following PH *in vivo*.

2.3. AOPP induced S-phase arrest of hepatocytes in vivo and in vitro

Flow cytometry (FCM) analysis showed that AOPP induced S-phase arrest in rat hepatocytes. The hepatocyte numbers in S-phase increased in the AOPP group, peaked at postoperative day 1 (30.28%), and remained at 14.96% for up to 7 days postoperatively (Fig. 3A). AOPP-induced S-phase arrest was accompanied by a significant decrease in G2-M phase numbers, which resulted in the suppression of hepatocyte division.

Cultured cell lines HL-7702 and AML-12 were incubated with the indicated concentration of AOPP for the controlled time periods. As shown in Fig. 3B-E, AOPP treatment induced S-phase arrest in a dose-dependent and time-dependent manner in both cell lines. In HL-7702 cells, AOPP caused a gradual increase of cell numbers in S-phase and a corresponding decrease in the G1 cell population between 24 h and 72 h. In AML-12 cells, AOPP-induced S-phase cell accumulation was accompanied by a decrease in G2-M phase cell numbers from 12 h to 48 h. To further investigate the effect of AOPP on cell proliferation, we analyzed cell proliferation with the cell counting kit-8 (CCK-8) assay and found that AOPP treatment inhibited cell proliferation in a time-dependent manner in both cell lines (Supplemental Fig. 2).

2.4. AOPP-induced S-phase arrest via NADPH oxidase-dependent ROS production in vivo and in vitro

ROS generation in response to the administration of AOPP was initially examined *in vivo*. Dichlorofluorescein (DCF) fluorescence in the FITC/FL-1 channel of the flow cytometer was used to assess ROS generation. Intracellular ROS generation in hepatocytes of remnant liver was significantly increased in AOPP-injected rats compared with that in controls and RSA-treated rats following PH ($P < 0.01$ at all time points) (Supplemental Fig. 3A). When rats were treated with NAC, an inhibitor of ROS, S-phase arrest in hepatocytes induced by AOPP treatment was significantly improved following PH ($P < 0.05$ at days 1 and 3; $P < 0.01$ at days 5 and 7).

Intracellular ROS generation was significantly enhanced in AOPP-treated HL-7702 and AML-12 cells ($P < 0.05$). As shown in Fig. 4A and B, incubation of HL-7702 and AML-12 cell cultures with AOPP induced

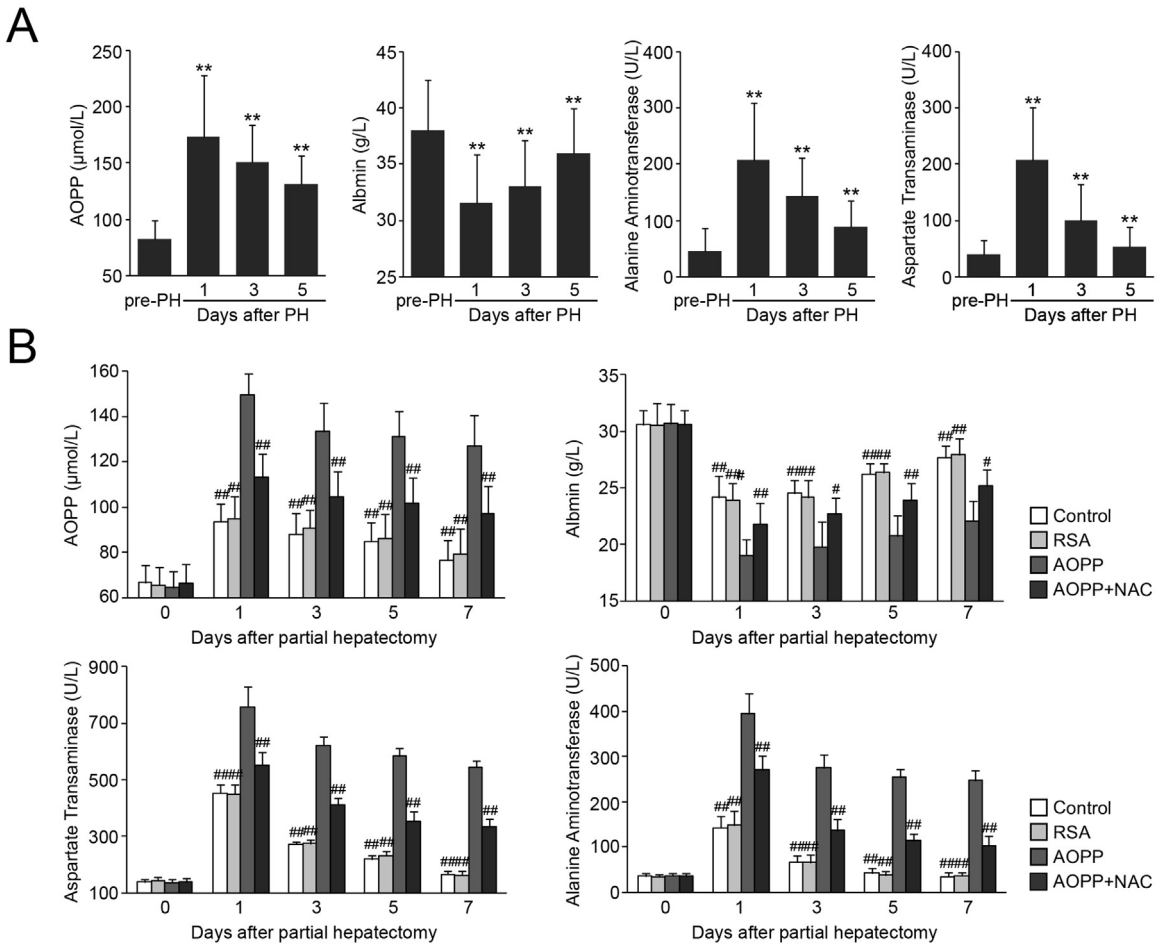

Fig. 1. Serum levels of AOPP and biochemical parameters in perioperative period of partial hepatectomy (PH) in human and animal subjects. (A) Changes of serum levels of AOPP and biochemical parameters after partial hepatectomy in human subjects. $^{*}P < 0.05$ versus pre-partial hepatectomy (pre-PH). $^{**}P < 0.01$ versus pre-PH. (B) AOPP treatment increased serum level of AOPP, alanine aminotransferase (ALT), Aspartate transaminase (AST) and decrease serum level of albumen (ALB) at indicated times after partial hepatectomy in rats. The changes of serum levels of AOPP and biochemical parameters were improved by *N*-acetylcysteine (NAC; 200 mg/kg) treatment. Data are presented as mean ± S.D. (n = 6). $^{\#}P < 0.05$ versus AOPP. $^{\#\#}P < 0.01$ versus AOPP.

a time-dependent and dose-dependent increase in ROS generation. Furthermore, AOPP-induced intracellular ROS generation, and S-phase arrest was almost completely blocked by pretreating with the ROS scavenger NAC in both cell lines (Fig. 4A-D), suggesting that AOPP-induced S-phase arrest in cultured hepatocytes was dependent on the generation of intracellular ROS.

Our previous study showed that NADPH oxidase was a critical step in AOPP-induced intracellular ROS production in intestinal epithelial cells [22]. To examine the mechanism underlying the induction of ROS generation in hepatocytes, we investigated NADPH oxidase activity in AOPP-treated HL-7702 and AML-12 cells. A co-immunoprecipitation assay showed that AOPP promoted the interaction of $p22^{phox}$ with NADPH oxidase membrane subunits NOX1 and NOX4 (Fig. 5A and B), but not NOX2 (data not shown), in both cell lines. Similarly, activation of NADPH oxidase in the hepatocytes of AOPP-challenged rats was also found *in vivo* (Supplemental Fig. 3B).

To further confirm whether this step was also required for the AOPP-induced ROS generation in hepatocytes, we pretreated the cultured cells with Nox1and Nox4 siRNA. As shown in Fig. 5C-F, Nox1 and Nox4 siRNA transfection dramatically decreased Nox1 and Nox4 expression and significantly reduced AOPP-induced intracellular ROS production in HL-7702 and AML-12 cells. Taken together, these data indicated that AOPP-induced intracellular ROS production was mainly mediated by the NADPH oxidase signaling pathway.

2.5. AOPP challenge downregulated β-catenin expression in vivo and in vitro

As shown in Fig. 6, immunohistochemistry showed that the staining intensity of β-catenin increased at 15 min and peaked at 30 min following PH in the livers of vehicle-treated or RSA-treated rats. Immunostaining for β-catenin was significantly lower in AOPP-treated rats compared with that in controls ($P < 0.01$ at 15 mins, 30 mins, and 24 h following PH). Intervention with the use of NAC prevented the decrease of β-catenin expression at the last four time points.

To validate the above findings, we investigated the effect of AOPP on β-catenin expression *in vitro*. Quantitative polymerase chain reaction (qPCR) showed that AOPP treatment inhibited β-catenin mRNA expression levels as early as 15 min in both cell lines (Fig. 7A). Meanwhile, Western blotting analysis also showed that AOPP treatment triggered a reduction in nuclear β-catenin expression at 30 min and 15 min in HL-7702 cells and AML-12 cells, respectively (Fig. 7B). In the cytoplasmic fraction, the decrease in β-catenin expression took place at approximately the same time as that of nuclear expression. Furthermore, Western blotting and immunofluorescence analysis showed that decreased β-catenin expression induced by AOPP was significantly prevented by pretreatment with NAC (Fig. 7C and Fig. 8), which suggested that AOPP-induced β-catenin downregulation in hepatocytes was mainly mediated by ROS production.

To further verify that AOPP-induced S-phase arrest was β-catenin-dependent, HL-7702 and AML-12 cells were transfected with lentivirus-

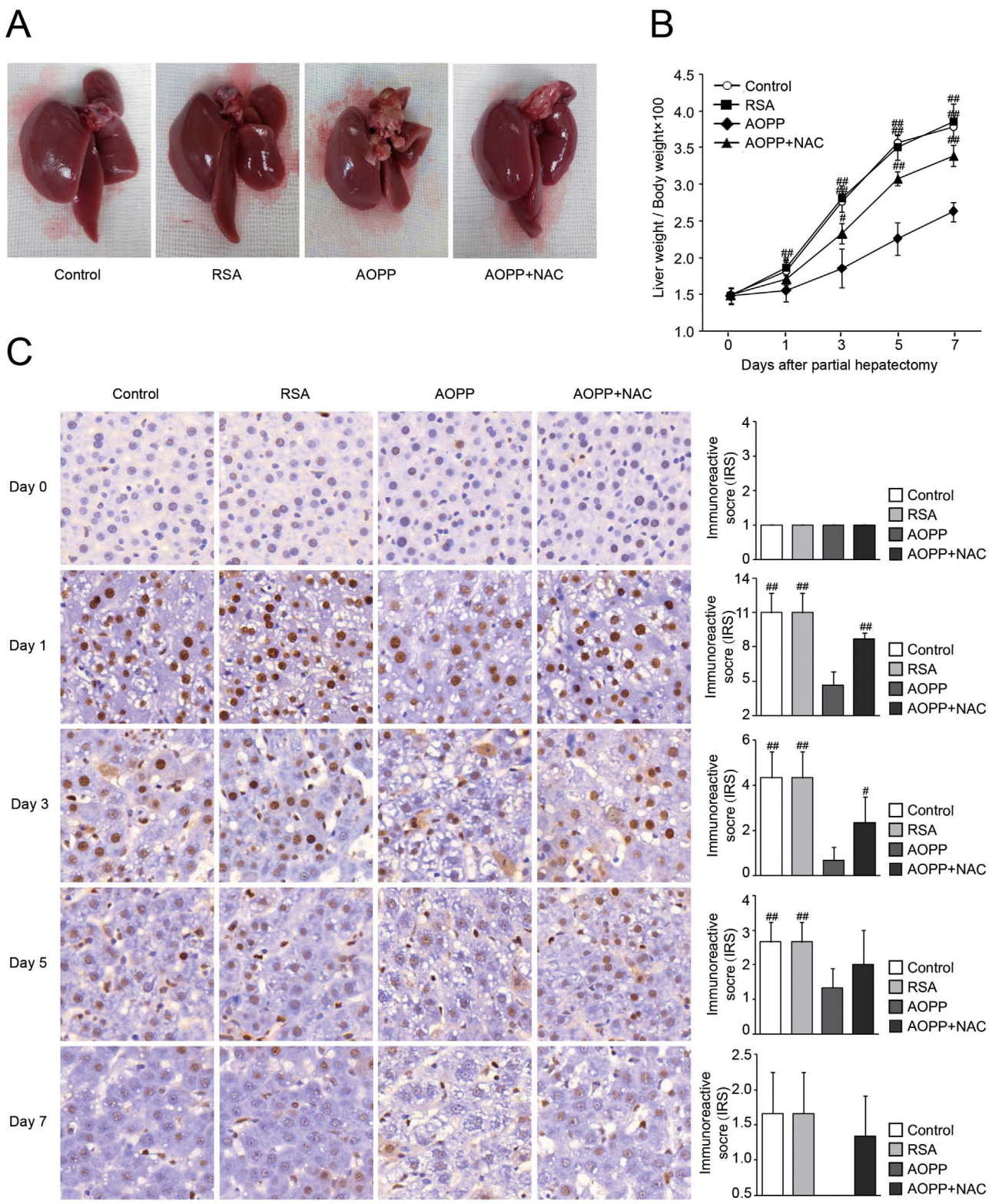

Fig. 2. Impaired liver regeneration in advanced oxidation protein products (AOPP)-treated rats after partial hepatectomy. (A) Livers of rats in four groups at day 7 after partial hepatectomy. (B) The liver weight to body weight ratio of rats in the four groups was assessed at the indicated time points after partial hepatectomy.(C) Immunohistochemical detection of proliferating cell nuclear antigen (PCNA) expression at indicated times after partial hepatectomy in remnant liver of rats. The immunoreactive scores (IRS) were also assessed. Data are presented as mean ± S.D. (n = 6). $^{\#}P < 0.05$ versus AOPP. $^{\#\#}P < 0.01$ versus AOPP.

encoding β-catenin (LV-β-catenin) followed by AOPP treatment. The interfering efficiency of lentiviral vector was detected by Western blot, and β-catenin expression in both cell lines were significantly enhanced after lentiviral vector transfection (Fig. 7D). As shown in Fig. 7E, AOPP-induced S-phase arrest was ameliorated by overexpression of β-catenin in both cell lines ($P < 0.05$). These observations indicated that down-regulation of β-catenin was a key event which required for AOPP-induced hepatocyte S-phase arrest during liver regeneration following PH.

Western blotting was also performed to examine the

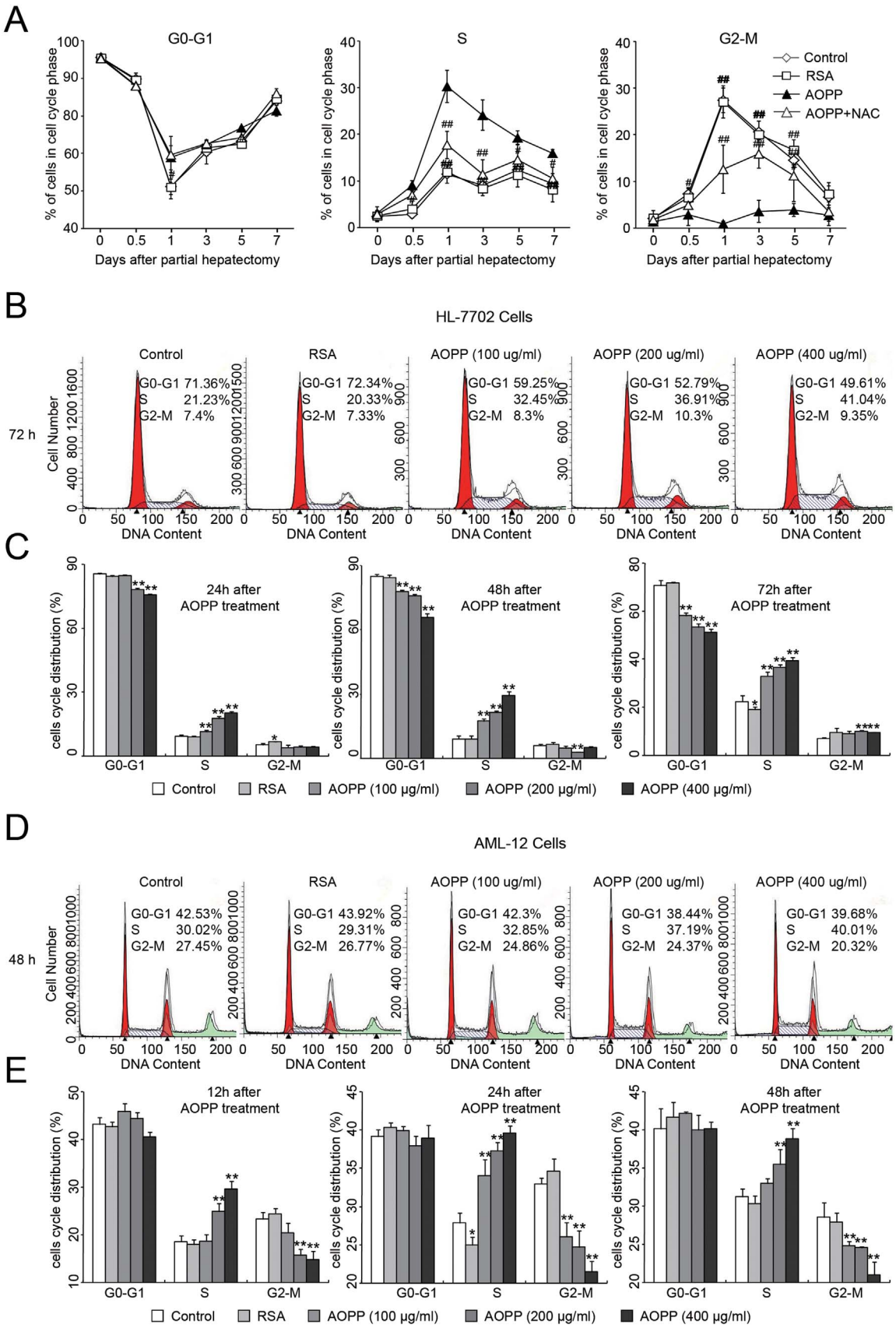

Fig. 3. Cell cycle analysis of hepatocytes after treatment with advanced oxidation protein products (AOPP) *in vivo* and *in vitro*. (A) Hepatocytes of remnant liver in rats were collected at indicated times after partial hepatectomy and analyzed by flow cytometry. The data indicated the percentage of cells in each phase of the cell cycle. The line chart showed that AOPP treatment induced S-phase arrest of hepatocytes *in vivo*. HL-7702 cells and AML-12 cells were treated with the indicated concentration of AOPP or native rat serum albumin (RSA) for the indicated time period. Representative diagrams of cell cycle distribution show S-phase arrest in the AOPP-treated HL-7702 cells (B) and AML-12 cells (D) compared with vehicle- or RSA-treated cells. AOPP induced S-phase arrest in HL-7702 cells (C) and AML-12 cells (E) at the indicated time points. Data are presented as mean ± S.D. $^{*}P < 0.05$ versus control. $^{**}P < 0.01$ versus control. $^{\#}P < 0.05$ versus AOPP. $^{\#\#}P < 0.01$ versus AOPP.

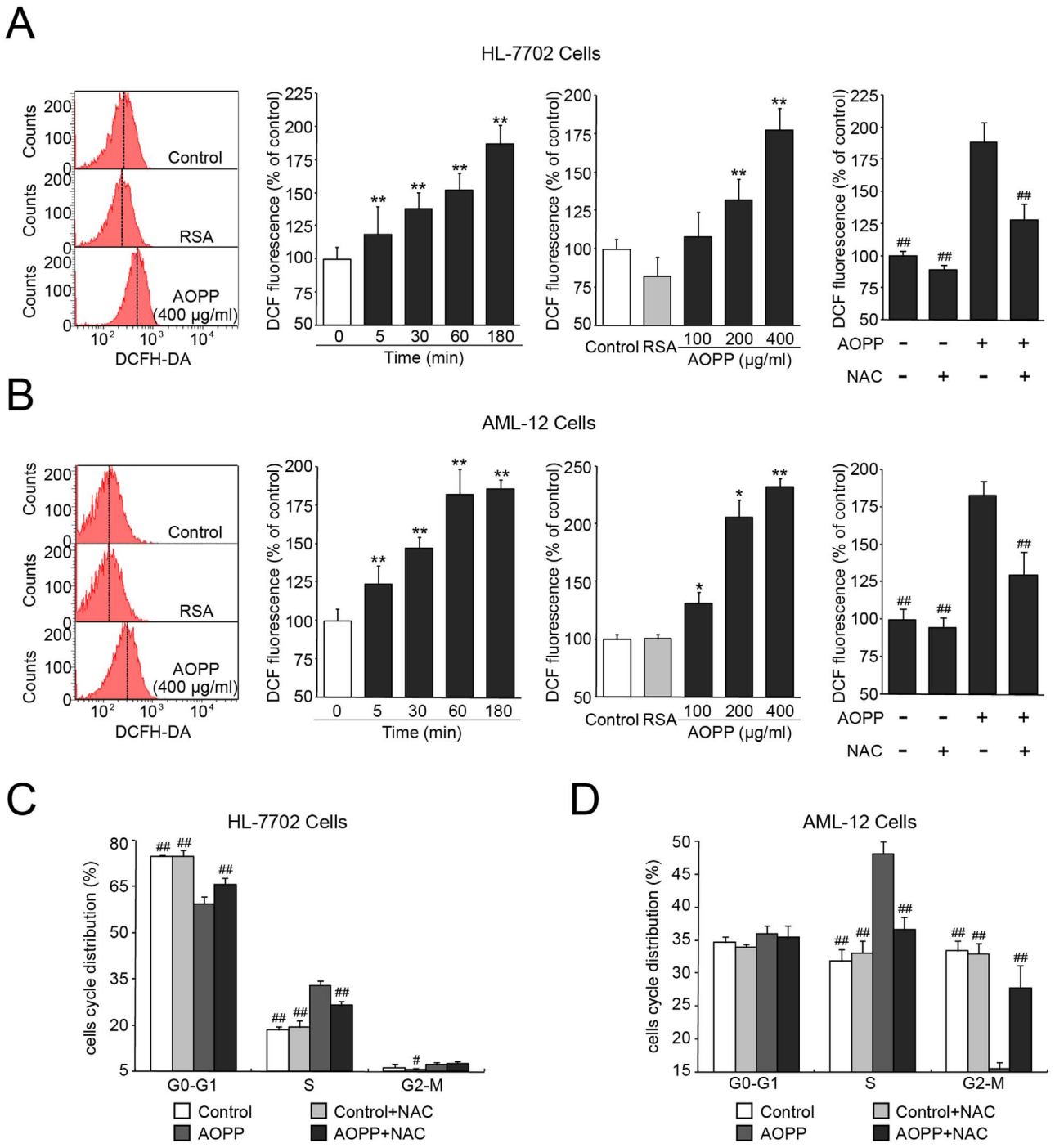

Fig. 4. Advanced oxidation protein products (AOPP)-induced S-phase arrest via reactive oxygen species (ROS) production. (A, B) Incubation of HL-7702 and AML-12 cultures with AOPP induced dose- and time-dependent increase in ROS generation, and AOPP-induced ROS production was significantly decreased by pretreatment with ROS scavenger *N*-acetylcysteine (NAC) (20 μM). (C, D) HL-7702 and AML-12 cells were pretreated with N-acetylcysteine (NAC) (20 μM) followed by treatment with AOPP. The S-phase arrest was largely blocked by pretreating with NAC (20 μM) in both cell lines. Data are presented as mean ± S.D. $^{*}P < 0.05$ versus control. $^{**}P < 0.01$ versus control. $^{\#}P < 0.05$ versus AOPP. $^{\#\#}P < 0.01$ versus AOPP.

phosphorylation of the JNK, ERK, and p38/MAPK signaling pathways in HL-7702 and AML-12 cells after AOPP treatment. AOPP could only activate the JNK signaling pathway through phosphorylation of the JNK1/2 protein in AML-12 cells (Supplemental Fig. 4A, B). However, pretreatment with JNK inhibitor (SP600125) did not prevent AOPP-triggered S-phase arrest (Supplemental Fig. 4C). These results indicated that AOPP-induced S-phase arrest was independent of the MAPK pathway in HL-7702 and AML-12 cells.

2.6. AOPP challenge downregulated cyclin-dependent kinase 2 (CDK2) expression in vivo and in vitro

It has previously been reported that the CDK2/cyclin A complex formed by CDK2 binding with cyclin A is required during S-phase of the cell cycle [32]. We further analyzed whether CDK2 or cyclin A was involved in AOPP-induced S-phase arrest *in vitro*. qPCR analysis and Western blotting showed that AOPP induced a reduction in CDK2 expression both in HL-7702 and AML-12 cells in a time-dependent fashion

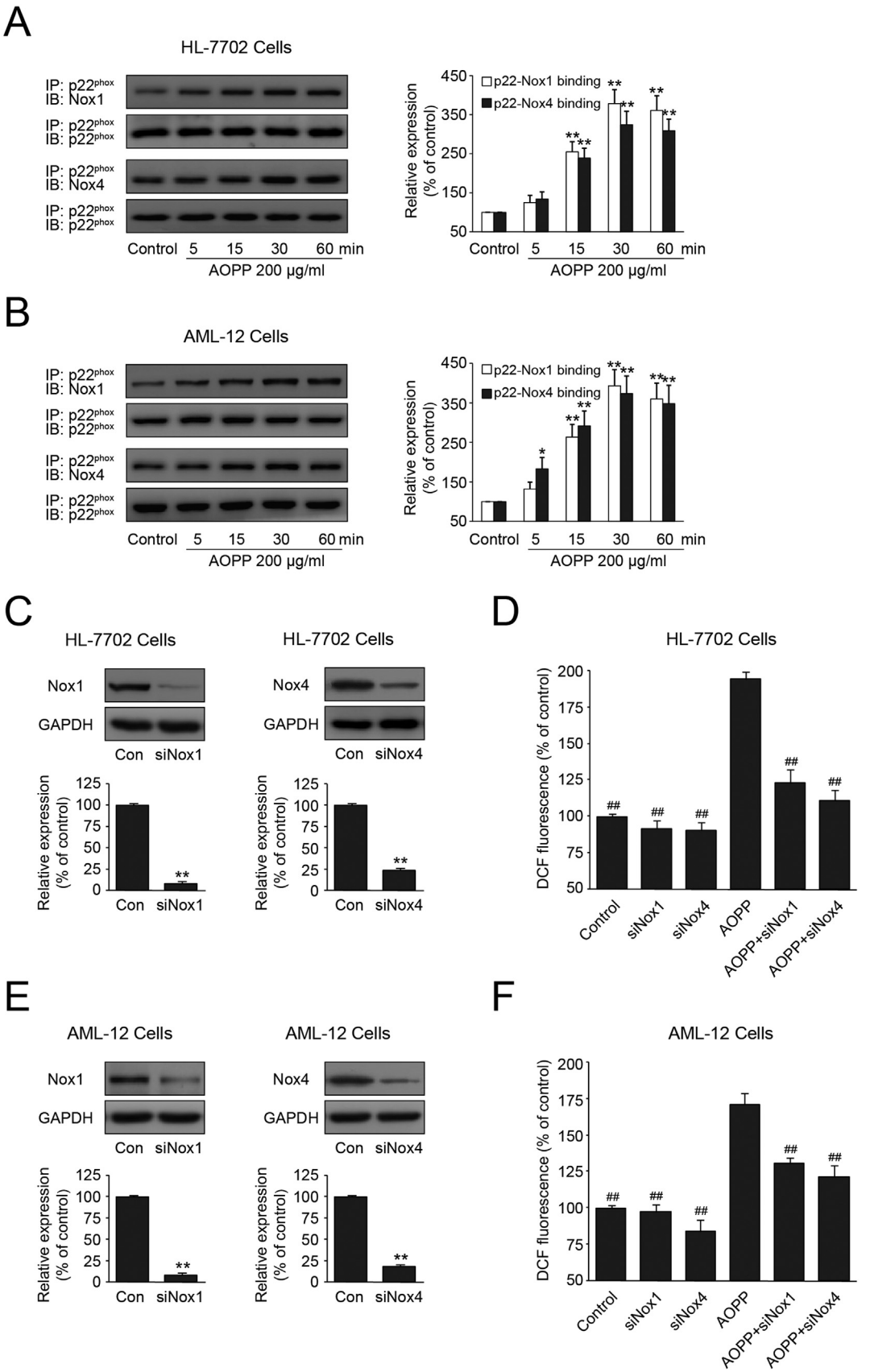

Fig. 5. Advanced oxidation protein products (AOPP) induced nicotinamide adenine dinucleotide phosphate (NADPH) oxidase-dependent reactive oxygen species (ROS) generation. (A, B) Results of co-immunoprecipitation analysis showed that AOPP treatment enhanced the binding of Nox1 or Nox4 to p22phox in HL-7702 and AML-12 cells. (C, E) The interfering efficiency of siNox1 and siNox4 were detected by Western blot, expression of Nox1 and Nox4 in HL-7702 and AML-12 cells were reduced after siRNA transfection. (D, F) ROS generation triggered by AOPP was decreased by transfection with siNox1 and siNox4. Data are presented as mean ± S.D. $^{*}P < 0.05$ versus control. $^{**}P < 0.01$ versus control. $^{\#}P < 0.05$ versus AOPP. $^{\#\#}P < 0.01$ versus AOPP.

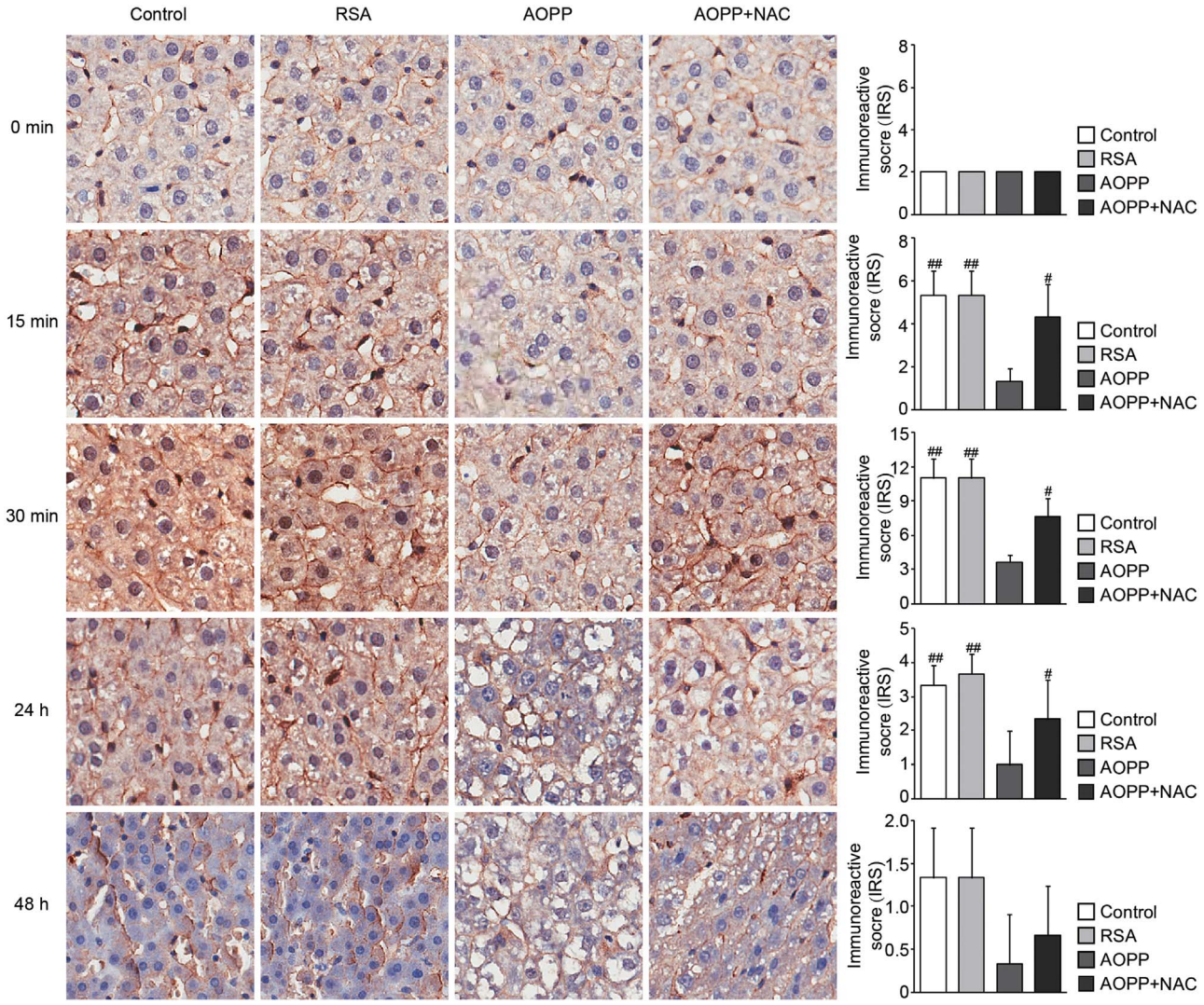

Fig. 6. Immunohistochemical detection of β-catenin expression at indicated times after partial hepatectomy (PH) in remnant liver of rats. The decrease of β-catenin expression was detected in advanced oxidation protein products (AOPP)-challenged rats and was ameliorated by *N*-acetylcysteine (NAC; 200 mg/kg) treatment. The immunoreactive scores were also assessed. Data are presented as mean ± S.D. (n = 6). $^{\#}P < 0.05$ versus AOPP. $^{\#\#}P < 0.01$ versus AOPP.

(Fig. 9A and B). CDK2 expression in HL-7702 and AML-12 cells decreased at 2 h after AOPP treatment. Following CDK2 alteration, the expression of cyclin A began to decrease after 12 h in both cell lines (Supplemental Fig. 5). AOPP administration decreased the formation of cyclin A/CDK2 complexes (Fig. 9C), corresponding to the time of CDK2 downregulation.

Overexpression of β-catenin by transfection with lentivirus-encoding β-catenin (LV-β-catenin) could reverse the decreased CDK2 expression in both cell lines on exposure to AOPP as early as 4 h (Fig. 9D). Whereas, in response to the overexpression of β-catenin, recovery of cyclin A expression took place at 12 h in AOPP-treated cell lines (data not shown). In addition, Western blotting analysis also showed that the decline of CDK2 expression induced by AOPP stimulation could be prevented by pretreatment with NAC (Fig. 9E). Since AOPP stimulation induced S-phase arrest accompanied by a decrease in G0-G1 phase cell populations in HL-7702 cells and a reduction in G2-M phase cell populations in AML-12 cells, we further assessed the effect of AOPP on special cyclin proteins involved in the regulation of G0-G1 and G2-M phase of the cell cycle. As shown in Supplemental Fig. 5, AOPP treatment also resulted in decreases in the level of cyclin D1 in HL-7702 cells and in the level of cyclin B in AML-12 cells in a dose-dependent manner, whereas cyclin E protein levels were without any noticeable change in both cell lines.

Immunohistochemical analysis of CDK2 expression in rat hepatocytes (Fig. 10) showed that the staining intensity of CDK2 increased at 6 h and peaked at 12 h after PH in the livers of vehicle-treated or RSA-treated rats. Consistent with the *in vitro* study, the downregulation of CDK2 was induced by AOPP administration and was prevented by pretreatment with NAC. These findings supported the hypothesis that AOPP-induced hepatocyte S-phase arrest was mediated by the ROS-β-catenin-CDK2 pathway.

3. Discussion

Advanced oxidation protein products (AOPP) are a family of dityrosine-containing protein products formed during excessive production of oxidants and carried mainly by albumin *in vivo* [33]. Recent studies have shown the accumulation of plasma AOPP in liver cirrhosis and hepatic failure [12,34]. However, little is known about the pathogenic role and mechanism of AOPP in liver disease. The present study has shown the enhanced formation of AOPP in patients undergoing partial hepatectomy (PH) for benign and malignant liver disease. We have also provided both *in vivo* and *in vitro* data to support that AOPP induced the occurrence of hepatocyte S-phase arrest via a ROS-dependent pathway involving the downregulation of β-catenin and CDK2. This preliminary study is, to our knowledge, the first to report AOPP accumulation as a

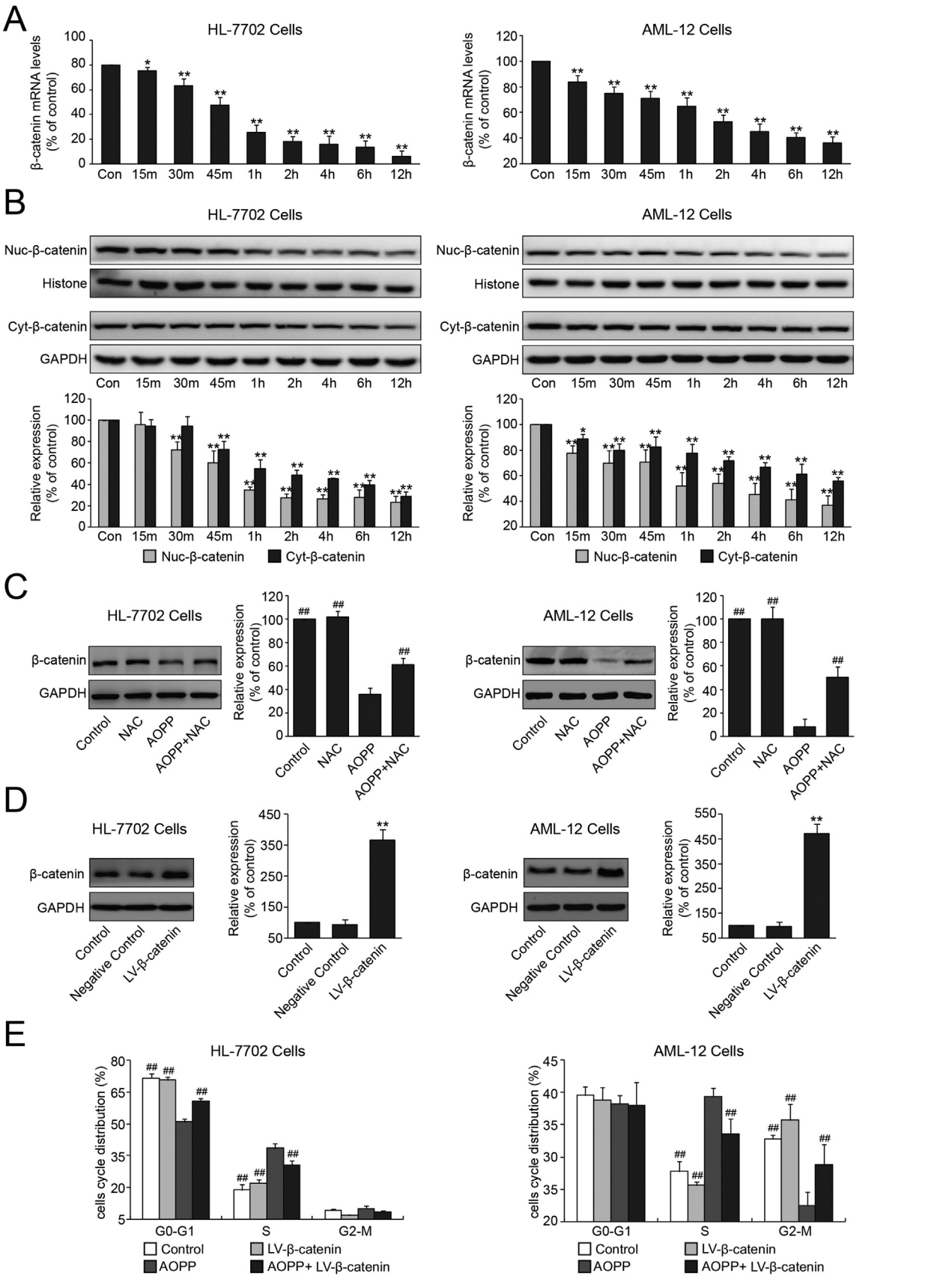

(caption on next page)

Fig. 7. Role of β-catenin in S-phase arrest of HL-7702 and AML-12 cell lines in response to advanced oxidation protein products (AOPP) treatment. (A) HL-7702 and AML-12 cells were treated with AOPP for the indicated times and quantitative polymerase chain reaction (qPCR) analysis was performed to assess the mRNA expression of β-catenin. (B) HL-7702 and AML-12 cells were treated with AOPP for the indicated times and western blot analysis was performed to assess the nuclear and cytoplasmic expression of β-catenin. Histone and glyceraldehyde-3-phosphate dehydrogenase (GAPDH) were used as nuclear and cytosolic marker proteins, respectively. (C) HL-7702 and AML-12 cells were pretreated with *N*-acetylcysteine (NAC; 20 μM), followed by treatment with AOPP for 12 h. Western blot analysis was performed to assess total expression of β-catenin. The decreased β-catenin expression induced by AOPP treatment was largely relieved by pretreating with NAC in both cell lines. (D) HL-7702 cells and AML-12 cells were transfected with lentivirus-encoding β-catenin (LV-β-catenin). The interfering efficiency of lentiviral vector was detected by Western blot analysis. (E) HL-7702 and AML-12 cells were pretreated with N-acetylcysteine (NAC) (20 μM) followed by treatment with AOPP. The S-phase arrest was largely blocked by pretreating with NAC in both cell lines. Cell cycle distribution was quantified by flow cytometry. Data are presented as mean ± S.D. $^{*}P < 0.05$ versus control. $^{**}P < 0.01$ versus control. $^{\#}P < 0.05$ versus AOPP. $^{\#\#}P < 0.01$ versus AOPP.

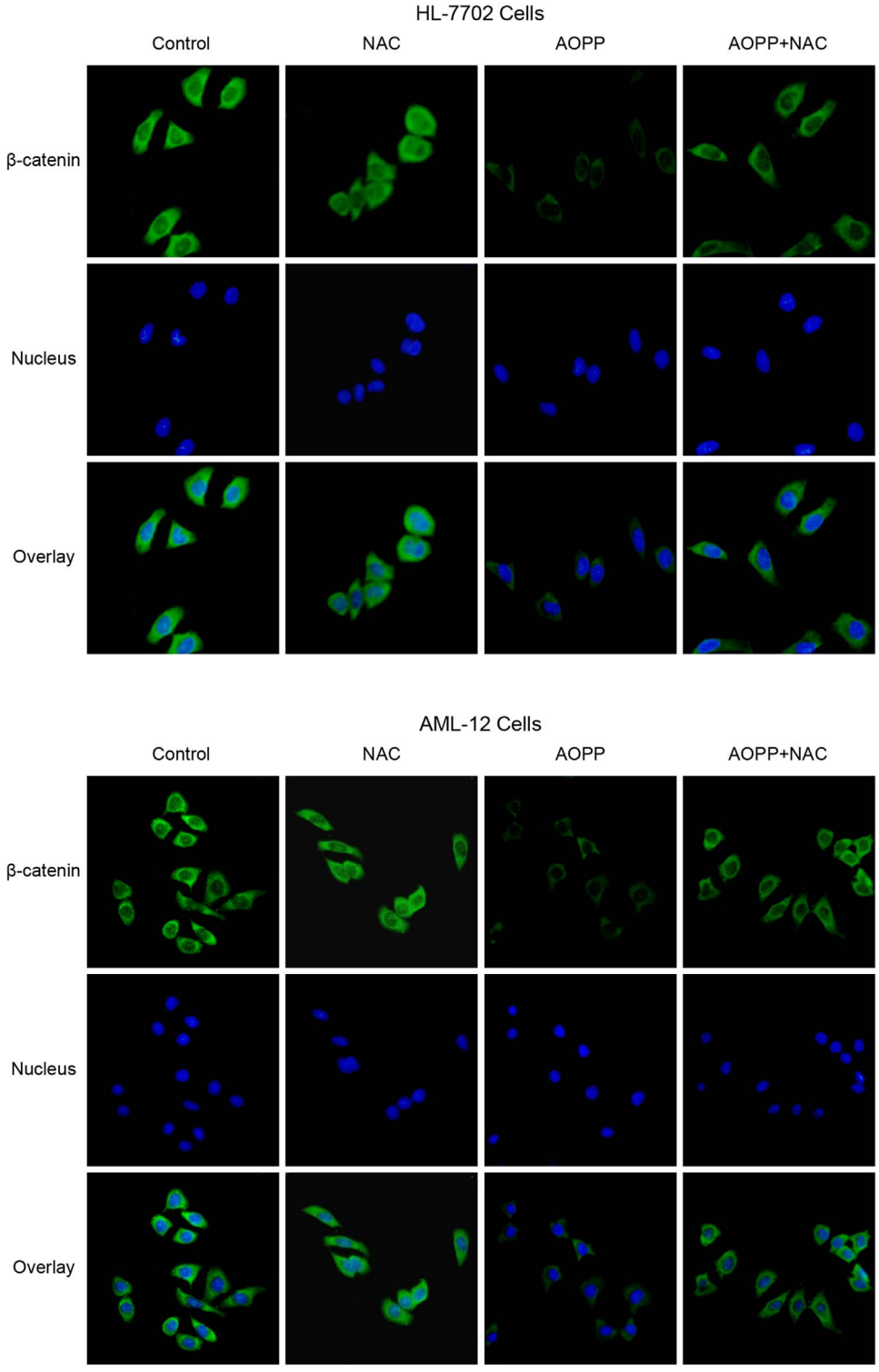

Fig. 8. β-catenin expression in advanced oxidation protein products (AOPP)-treated HL-7702 and AML-12 cell lines. HL-7702 and AML-12 cells were incubated with an anti-β-catenin antibody after 6 h treatment of phosphate buffer saline (PBS) with or without pretreatment with reactive oxygen species (ROS) scavenger *N*-acetylcysteine (NAC; 20 μM) for 1 h or AOPP with or without pretreatment with NAC (20 μM) for 1 h, then incubated with Alex 555-conjugated secondary antibody, and counterstained with 4',6-diamidino-2-phenylindole (DAPI). The change in β-catenin expression is demonstrated by the overlap of β-catenin and nuclear staining.

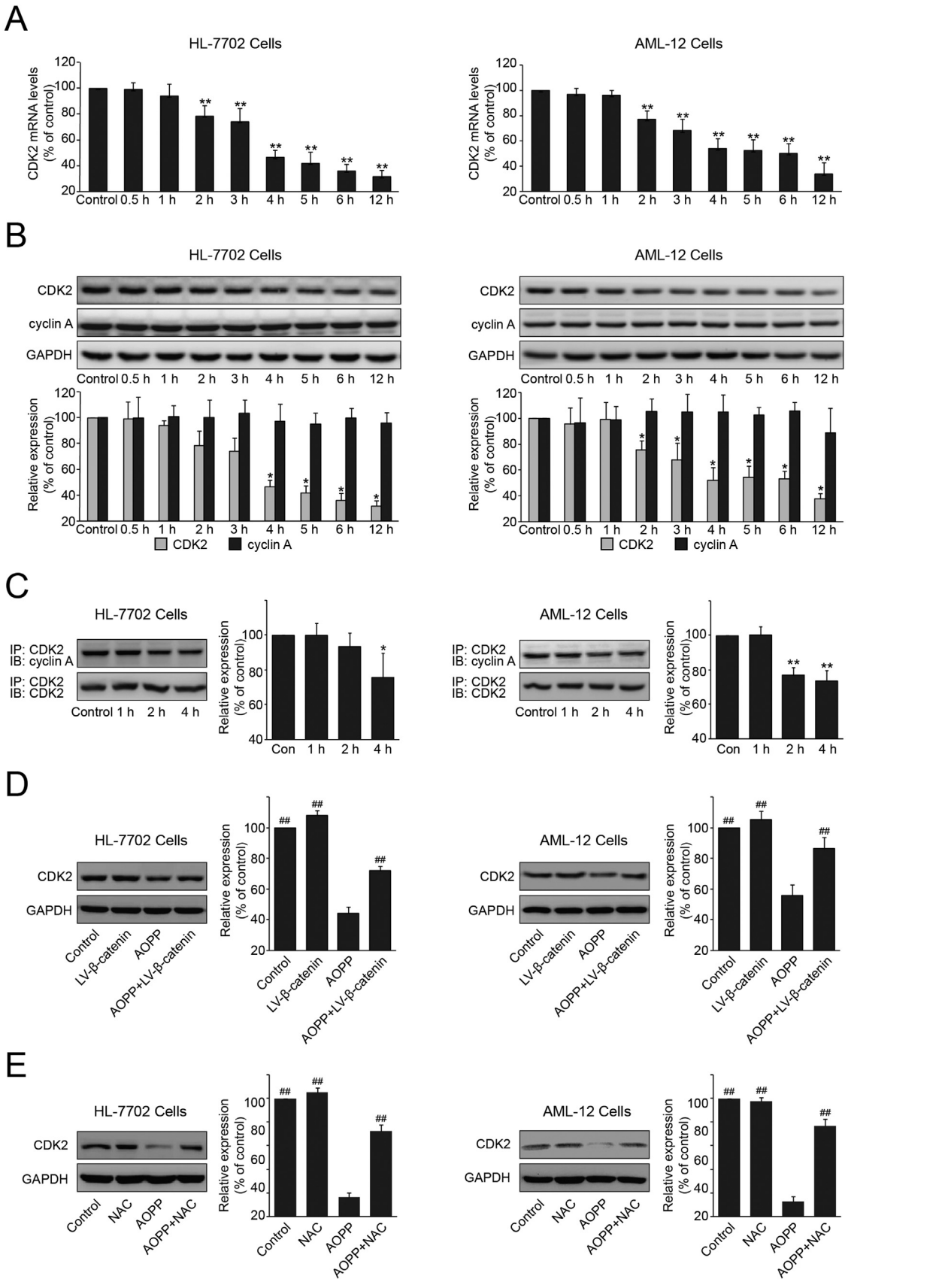

(caption on next page)

Fig. 9. Role of CDK2 in S-phase arrest of HL-7702 and AML-12 cell lines in response to advanced oxidation protein products (AOPP) treatment. (A) HL-7702 and AML-12 cells were treated with AOPP for the indicated times and quantitative polymerase chain reaction (qPCR) analysis was performed to assess the mRNA expression of CDK2. (B) HL-7702 and AML-12 cells were treated with AOPP for the indicated times and western blot analysis was performed to assess the expression of CDK2 and cyclinA. Histone and glyceraldehyde-3-phosphate dehydrogenase (GAPDH) were used as marker proteins. (C) HL-7702 cells and AML-12 cells were treated with AOPP for 4 h. Interactions between CDK2 and cyclin A were analyzed by co-immunoprecipitation. (D) HL-7702 and AML-12 cells were transfected with lentivirus-encoding β-catenin (LV-β-catenin) followed by AOPP treatment. Representative Western blots and densitometry quantification revealed that the decrease of CDK2 expression and the complex formation was relieved in LV-β-catenin cells. (E) Representative Western blots and densitometry quantification revealed that the decreased CDK2 expression induced by AOPP treatment was largely relieved by pretreating with *N*-acetylcysteine (NAC; 20 μM) in both cell lines. Data are presented as mean ± S.D. $^{*}P < 0.05$ versus control. $^{**}P < 0.01$ versus control. $^{\#}P < 0.05$ versus AOPP. $^{\#\#}P < 0.01$ versus AOPP.

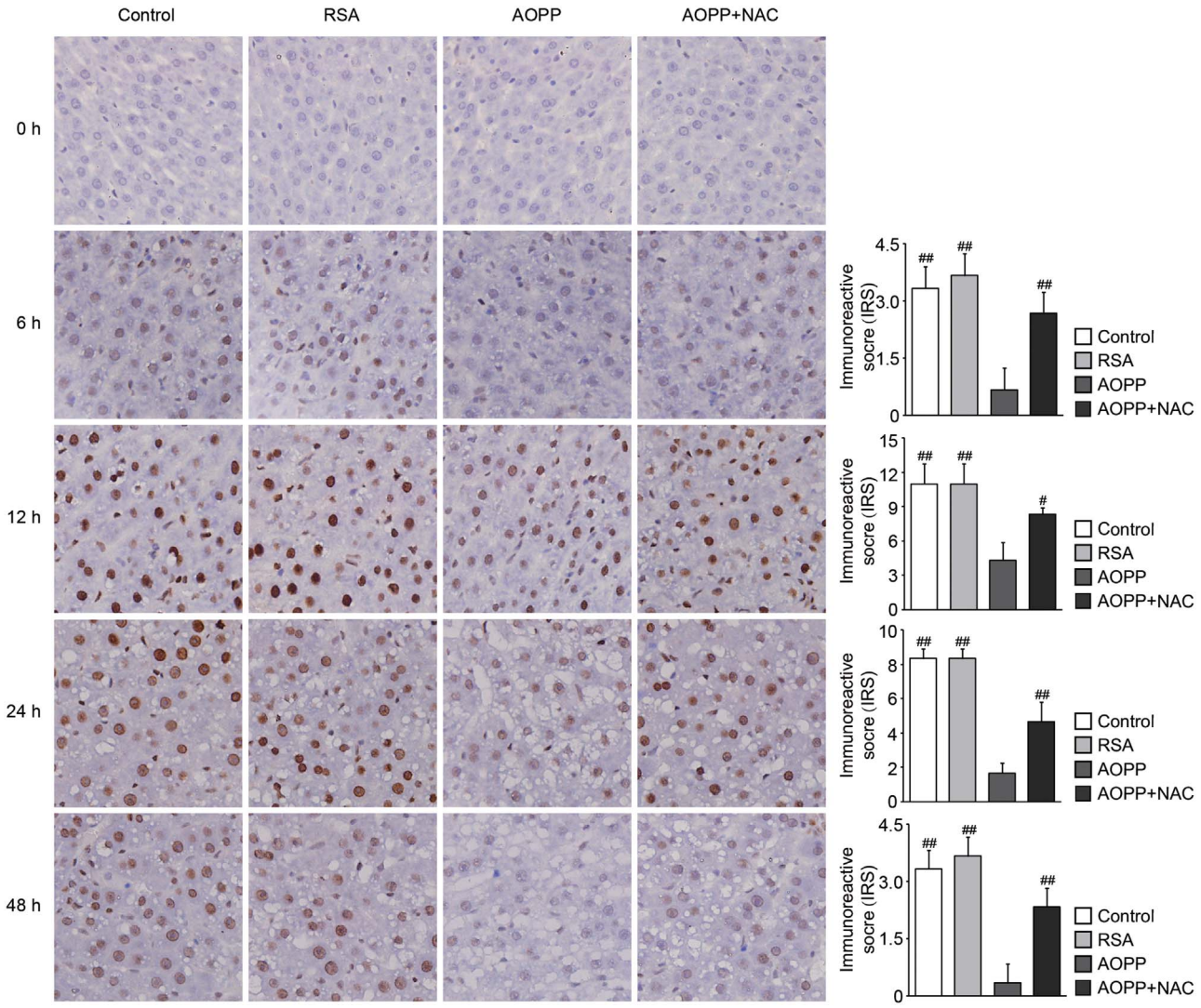

Fig. 10. Immunohistochemical detection of CDK2 expression at indicated times after partial hepatectomy (PH) in remnant liver of rats. The decrease of CDK2 expression was detected in advanced oxidation protein products (AOPP)-challenged rats and was improved by treatment with *N*-acetylcysteine (NAC) 200 mg/kg. The immunoreactive scores were also assessed. Data are presented as mean ± S.D. (n = 6). $^{\#}P < 0.05$ versus AOPP. $^{\#\#}P < 0.01$ versus AOPP.

novel mechanism for S-phase arrest in hepatocytes, and to confirm the pathogenic effect of AOPP on liver regeneration.

Oxidative stress is a common feature of surgical trauma [35,36]. Under such conditions, plasma proteins are prone to oxidation by chlorinated oxidants to form advanced oxidation protein products (AOPP). In this study, serum levels of AOPP as the marker of oxidative stress significantly increased even though serum albumin, the major source of AOPP production, decreased in patients following PH. Furthermore, responding to AOPP treatment following PH, the serum levels of ALT and AST significantly increased, and the liver mass remarkably reduced. Combined with our clinical data, these observations further confirmed the involvement of AOPP in hepatocytes damage and may subsequently participate in liver regeneration impairment. The mechanisms by which AOPP slowed liver regeneration remain to be clarified.

Liver regeneration following PH is mainly contributed by hepatocyte proliferation based on a proper progression of the hepatocyte mitotic cell cycle [37,38]. Our *in vivo* study found that AOPP resulted in hepatocyte cell cycle arrest in S-phase, and revealed a similar effect of AOPP on S-phase arrest in both HL-7702 and AML-12 cells. Because of differences in cell cycle length in various cell lines, the S-phase arrest in AML-12 cells occurred earlier than that in HL-7702 cells.

Previous studies have shown that ROS production mediates intracellular signaling activation in many biological processes [39,40]. Our previous study identified that AOPP accumulation in rat intestines resulted in excessive ROS production and decreased antioxidant system activity [18,22]. Therefore, one issue worth investigating was whether oxidative stress was responsible for AOPP-induced hepatocyte S-phase

arrest. This study indicated that AOPP administration triggers ROS production in hepatocytes *in vivo* and *in vitro*. Our results were consistent with recent data obtained with Nrf2 knockout mice, which demonstrated a causal role of ROS in impaired liver regeneration [17]. We further deciphered the intracellular signaling responsible for the triggering effect of AOPP on ROS production. Previous reports have demonstrated that nicotinamide adenine dinucleotide phosphate (NADPH) oxidase represented the major source of ROS generation and played a pivotal role as the modulator in ROS-mediated oxidative damage in various cell types [22,41]. In this study, we provided evidences demonstrating that AOPP-triggered ROS generation was dependent on NADPH oxidase. First, AOPP increased binding of homologs of the cytochrome subunit of the phagocyte NADPH oxidase Nox1 and Nox4 with membrane subunit p22phox, supporting the idea that hepatocyte Nox proteins are likely to act as endogenous sources of ROS generation during AOPP-induced pathogenesis [42,43]. Second, Blocking NADPH oxidase activity effectively attenuated AOPP-induced ROS production, indicating that NADPH oxidase was the major source of ROS challenged by AOPP. These finding indicated that the NADPH oxidase-mediated ROS generation serving as the key factor to promotion of AOPP-induced S-phase arrest.

Liver regeneration is a complex phenomenon involving a concerted effort of a series of signaling pathways. Previous studies have described that an initial increase of nuclear level of β-catenin during early liver regeneration favors its role in contributing toward initiation of hepatocytes proliferation [28,44]. In the present *in vivo* study, we demonstrated that AOPP treatment reduced the expression levels of total and nuclear β-catenin in rat liver following PH, which indicated that the compromise in regeneration was probably due to a lower β-catenin level especially in the cell nucleus [45]. Furthermore, overexpression of β-catenin due to lentivirus transfection alleviated hepatocyte S-phase arrest. Positive relation of β-catenin to hepatocyte proliferation during liver regeneration has been reported and thus our finding is in accordance with previous studies [46]. These indicated a direct role of β-catenin in AOPP-induced S-phase arrest. We also showed that the pretreatment with ROS scavenger NAC reversed the downregulation of β-catenin. These data suggested that the ROS-β-catenin pathway has a specific role in AOPP-induced S-phase arrest in hepatocytes. In addition, our results demonstrated that AOPP-induced S-phase arrest in HL-7702 and AML-12 cells was independent of MAPK signaling.

The cyclin A/CDK2 complex as an S-phase regulator, it particularly acts during the priming and progression of DNA synthesis [47]. Previous studies have reported that inhibition of CDK2 expression plays a role in the accumulation of cells in S-phase [48]. Conversely, upregulation of CDK2 has also been found to accompany S-phase arrest in HeLa cells [49]. These studies suggest that a mechanism for CDK2 in the regulation of S-phase arrest is plausible. In the present study, cell cycle analysis revealed a significant increase of hepatocytes in S-phase arrest following a rapid decrease in the CDK2 and cyclin A-CDK2 complex expression; the downregulation of cyclin A expression occurred much later in response to AOPP treatment in both cell lines. This suggested that CDK2 was implicated in the key molecular mechanisms that contributed towards S-phase arrest in hepatocytes. As expected, the triggering effect of AOPP on CDK2 downregulation was significantly inhibited by pretreatment with antioxidant NAC or β-catenin overexpression, supporting the idea that the ROS-β-catenin pathway was involved in AOPP-induced CDK2 downregulation of hepatocytes. D-type cyclins usually bind to CDK4 and to CDK6, and cyclin D/CDK4 complex is essential for G1-phase progression [50,51]. Our data showed that cyclin D1 expression in AML-12 cells was not altered after AOPP treatment. Despite the rapid decrease of cyclin D1 protein expression detected in HL-7702 cells, the HL-7702 cells were arrested in S-phase rather than in G1 phase in response to AOPP treatment. In both cultured hepatocyte cell lines, AOPP had no effect on cyclin E, which is a key protein in regulating cell cycle progression from G1 into S-phase [52]. We suggest that the reason for the absence of G1 arrest in HL-7702 cells was due largely to unimpaired cyclin E protein having a compensatory role that drove the hepatocytes to progress from G1 to S-phase. Also, cell mitosis is mainly regulated by cyclin B in complex with CDK1 in the G2-M phase [53]. Our data showed a significant reduction of cyclin B in AML-12 cells and an unchanged level of cyclin B in HL-7702 cells, which was consistent with the G2-M phase distribution of cell cycle testing by flow cytometry.

Taken together, our finds delineate an important role for AOPP in activating S-phase arrest in hepatocytes, which is mainly mediated by NADPH-dependent, ROS/β-catenin/CDK2-mediated pathway. On the basis of evidence presented in this report, we propose that AOPP may represent a novel pathogenic factor that contributes to liver regeneration impairment. This finding might be highly significant because it might be a central step toward the understanding the liver pathogenic effects of AOPP and may provide a new target for prevention of liver regeneration impairment after PH.

4. Materials and methods

4.1. Patients' studies

A total of 33 patients with histologically confirmed hepatocellular carcinoma were enrolled in the study. All patients underwent partial hepatectomy (PH) at Nanfang Hospital between August and December 2016. Patients with other coexisting severe systemic diseases or serious infection were excluded.

Venous blood samples taken in a fasting state were collected in sterile vacuum tubes before and 1, 3, and 5 days after the operation. Serum was obtained by centrifugation ($3000 \times g$, 10 min) of clotted blood and stored at −80 °C before measurement.

The study protocol was approved by the Medical Ethics Committee of Nanfang Hospital and was carried out according to the ethical principles of the World Medical Association (WMA). All patients who participated in the study gave the appropriate signed informed consent.

4.2. Advanced oxidation protein products (AOPP) determination

Advanced oxidation protein products (AOPP) concentration in serum was expressed in equivalents of chloramine-T and was assessed by using spectrophotometry, as described previously [22]. Briefly, 200 μL of serum samples (1:5 diluted in PBS), 200 μL of chloramine-T (Sigma, St. Louis, MO, USA) for calibration (0–100 μM) and 200 μL of phosphate buffered saline (PBS) as blank controls, were placed into a 96-well plate. Then, 10 μL of 1.16 M potassium iodide and 20 μL of acetic acid were added in turn. The absorbance of the reaction mixture at 340 nm was read immediately. The AOPP concentrations were expressed as micromoles per liter (μM/L) of chloramine-T equivalents [22].

4.3. AOPP preparation

AOPP were prepared *in vitro* by incubating rate serum albumin (RSA) (Sigma, St. Louis, MO, USA) with hypochlorous acid (Fluke, Buchs, Switzerland) as previously described [22]. AOPP in the preparations were determined with an OxiSelect AOPP Assay Kit (Cell Biolabs, San Diego, CA, USA). The content of AOPP was 50.10 ± 3.92 μmol/g protein in AOPP, and 0.22 ± 0.06 μmol/g protein in unmodified rate serum albumin (RSA).

4.4. Animal studies

All animal procedures were approved by the Laboratory Animal Care and Use Committee of Southern Medical University (Guangzhou, China). Male Sprague-Dawley (SD) rats, initial weight 180–200 g, (Southern Medical University Animal Experiment Center, Guangzhou, China) were maintained under standardized conditions with alternating

12 h dark/light cycles, and allowed free access to diet and water.

Partial hepatectomy (PH) was performed by removing 70% of the liver mass, as previously described [4]. After the operation, rats were randomly assigned to four experimental groups and received daily intravenous injections of vehicle (PBS, pH7.4), unmodified RSA (25 mg/kg per day), AOPP (25 mg/kg per day) and AOPP (25 mg/kg per day) + *N*-acetylcysteine (NAC) at 200 mg/kg; 30 min prior to AOPP for 7 days. The dosage of AOPP and the injection intervals were based on data from our preliminary experiment [22] and the rate of serum AOPP level increased in human cases that by this procedure, serum AOPP concentrations in the AOPP-treated group increased 1.0-fold at day 1 compared with that at day 0 after PH.

Hepatocytes isolated from the rats from each group, using a two-step collagenase perfusion technique, were collected for analysis of cell cycle distribution and intracellular reactive oxygen species (ROS) production at 0, 1, 3, 5 and 7 days after PH.

Rats were also sacrificed at same time points after PH by cervical dislocation under isoflurane anesthesia. Part of the liver tissue was fixed in 4% formaldehyde and embedded in paraffin wax, and 4 μm fixed tissue sections of liver were stained for morphologic and immunohistochemical examination.

4.5. Hematoxylin and eosin (H & E) and immunohistochemistry (IHC) staining

H & E and immunohistochemistry staining was performed according to the standard laboratory methods. The β-catenin antibody, used at a dilution of 1:200, was purchased from Cell Signaling Technology (Beverly, MA, USA). The AOPP antibody, used at a dilution of 1:100, was a gift from Professor Fu Ning (Southern Medical University, Guangzhou, China). The immunohistochemical localization of proteins within tissue sections was visualized as brown immunostaining using a standard diaminobenzidine protocol.

Each immunostained section was viewed under light microscopy and evaluated independently by two experienced pathologists. Immunoreactive scores (IRS) were the product of staining intensity (graded between 0 and 4, being 0 = negative, 1 = weakly positive, 2 = moderately positive, 3 = strongly positive) and the percentage of positively stained cells (graded between 0 and 4, being 1 = 0–25%, 2 = 26–50%, 3 = 51–75%, 3 = 76–100%).

4.6. Cell culture

The normal hepatocyte cell lines HL-7702 and AML-12 (Committee on Type Culture Collection, Chinese Academy of Sciences, Shanghai, China) were cultured at Roswell Park Memorial Institute (RPMI)-1640 supplemented with 10% fetal bovine serum (FBS) and in Dulbecco's modified Eagle medium (DMEM) supplemented with 10% FBS, respectively. The cells were incubated with 5% CO_2 and 95% humidity at 37 ˚C.

4.7. SiRNA transfection

Oligonucleotide siRNA duplex (Nox1, Nox4) was synthesized by Shanghai Gene Pharma (Shanghai, China).

The sequence of human Nox1 siRNA was CCAGGATTGAAGTGGATGG. The sequence of human Nox4 siRNA was ACUAUGAUAUCUUCUGGUA. The sequence of mice Nox1 siRNA was CAGAGGCAAGAGATCCATC. The sequence of mice Nox4 siRNA was GGUUACAGCUUCUACCUACUU. The transfection of siRNA in HL-7702 and AML-12 was carried out with Lipofectamine 3000 (Invitrogen, Carlsbad, CA, USA) according to the manufacturer's instructions.

4.8. Lentivirus transduction

The lentivirus-encoding β-catenin (LV-β-catenin), used to overexpress β-catenin and the empty vector (LV-normal control; LV-NC), were obtained from GeneCopoeia (Guangzhou, China). LV-β-catenin and LV-NC were transduced into HL-7702 and AML-12 cells. Briefly, in order to obtain efficient lentivirus transduction, primary HL-7702 or AML-12 cells were seeded in RPMI-1640 or DMEM with 10% fetal bovine serum for 24 h. The cells were transfected with lentivirus for 24 h, and then treated with AOPP for further analysis.

4.9. Flow cytometry analysis

To analyze the distribution of cell cycle stage, control and treated cells were collected, washed with PBS, and fixed with cold 70% ethanol overnight at 4 ˚C. The fixed cells were centrifuged, washed twice with ice-cold PBS, and resuspended in RNase A (50 g/ml) for 30 min, followed by incubation with propidium iodide (50 g/ml) staining solution for 30 min at room temperature. Cell cycle distribution was then measured using a flow cytometry (BD Biosciences, San Jose, CA, USA).

4.10. Cell proliferation assay

Cell proliferation was examined using the Cell Counting Kit-8 (CCK-8) (Dojindo, Kumamoto, Japan) assay according to the instructions from the supplier. Briefly, HL-7702 and AML-12 cells were placed in a 96-well plate at a density of 5×10^3 cells/well and 2×10^3 cells/well, respectively. Cells were allowed to adhere for 24 h at 37 ℃ and then treated with AOPP (200 μg/ml) for increasing times. Following treatment, CCK-8 reagent was added to each well, and the cells were incubated for 2 h at 37 ˚C. Immediately after the incubation, viable cells were detected by measuring absorbance at 450 nm using an absorbance microplate reader (Bio-Tek, Seattle, USA). Cell viability was expressed as percentage absorbance of cells treated with AOPP compared with the percentage absorbance of untreated cells.

4.11. Immunoprecipitation and Western blot

The interaction of cyclin with CDK in cultured hepatocytes was determined as previously described [54]. Briefly, the lysates fractionated by SDS-polacrylamide gel electrophoresis (PAGE) were electrotransferred to polyvinylidene fluoride membranes (Millipore, Billerica, MA, USA). Following blocking, the membranes were incubated with primary antibodies overnight at 4 ˚C. The protein bands were incubated with corresponding secondary antibodies and then detected with chemiluminescence detection reagents (Millipore). The following antibodies were used:, anti-CDK2 Ab, anti-β-catenin Ab, anti-Cyclin D1 Ab, anti-p-22 Ab, anti-Nox1 Ab, anti-Nox4 Ab, goat anti-mouse and goat anti-rabbit IgG-horseradish peroxidase (HRP) from Cell Signaling Technology (Beverly, MA, USA); anti-Cyclin A Ab, anti-Cyclin B Ab and anti-Cyclin E Ab were from ABclonal (Cambridge, MA, USA). All antibodies were used at a dilution of 1:1000. The anti-GAPDH Ab, used at a dilution of 1:3000, were from Boster (Wuhan, China). Relative quantification of protein levels was determined by measuring the intensity of the protein bands with the use of Gel-Pro Analyzer (Media Cybernetics, Sarasota, Florida, USA).

4.12. Real-time PCR

Total RNA was extracted using the TRIzol RNA isolation system (Takara, Dalian, China) according to the manufacturer's instructions. The first strand of complementary DNA was reverse transcribed using PrimeScript™ RT Master Mix (Takara, Dalian, China) and real-time quantitative polymerase chain reaction (qPCR) was performed using SYBR Green mix (Takara, Dalian, China). The following conditions were used for PCR: 95 ˚C for 30 s followed by 40 amplification cycles at 95 ˚C for 5 s and 60 ˚C for 20 s. The sequences of the primer pairs were given in Supplemental Table 1. Glyceraldehyde-3- phosphate dehydrogenase (GAPDH) gene was used as the internal normalization control. The

LightCycler 480 System (Roche, Basel, Switzerland) was used for determination of mRNA levels. The ratio of each transcript to glyceraldehyde 3-phosphate dehydrogenase (GAPDH) was calculated for each sample.

4.13. Immunofluorescence staining

HL-7702 and AML-12 cells were cultured on coverslips and fixed with cold methanol for 30 min, with or without permeabilization of 0.5% Triton X-100. The cells were then incubated with primary antibodies against β-catenin overnight at 4 ℃. Following incubation of primary antibodies, the cells were stained with Alexon 555-conjugated secondary antibodies (Invitrogen, Carlsbad, CA) and the nuclei were stained with DAPI. Intracellular location and expression were viewed using an Olympus XB-51 fluorescence inverted microscope (Olympus, Tokyo, Japan).

4.14. Measurement of ROS production

Intracellular ROS generation was assessed using the peroxide-sensitive fluorescent probe dichlorofluorescein diacetate (DCFH-DA) with a flow cytometer (Becton Dickinson, USA). Briefly, HL-7702 and AML-12 cells treated by AOPP and primary hepatocytes isolated from the remnant liver of rats in each group at the day 0, 1, 3, 5, 7 after PH were incubated with DCFH-DA at 37 ℃ for 30 min, washed twice with PBS and then resuspended in PBS to detect the generation of intracellular ROS by flow cytometry. To determine the source of ROS production, HL-7702 and AML-12 cells were pretreated for 60 min with ROS scavengers, *N*-acetylcysteine (NAC), 20 μM, and then incubated with 200 μg/ml AOPP for 30 min. The intracellular ROS generation was determined by dichlorofluorescein (DCF) fluorescence analysis.

4.15. Statistical analysis

All experiments were repeated at least three times. Data were expressed as mean ± standard deviation (SD). A two-tailed Student's *t*-test was used to compare means between two groups. Multiple comparisons were performed by one-way ANOVA, and pairwise comparisons were evaluated by the least significant difference (LSD) test or Dunnett's T3 method, where appropriate. Linear regression analysis was used to assess the correlation between AOPP and other biochemical parameters. Statistical analysis was performed with SPSS 13.0 (SPSS Inc, Chicago, IL, USA), and significance was defined as $P < 0.05$.

Acknowledgements

The work was supported by the National Key Clinical Specialty Discipline Construction Program, National Natural Science Foundation of China [grant number 81500398]; and Natural Science Foundation of Guangdong Province [grant number 2015A030310480].

Conflict of interest

The authors declare no conflict of interest.

Appendix A. Supplementary material

Supplementary data associated with this article can be found in the online version at http://dx.doi.org/10.1016/j.redox.2017.09.011.

References

[1] B. Nordlinger, H. Sorbye, B. Glimelius, G.J. Poston, P.M. Schlag, P. Rougier, et al., Perioperative chemotherapy with FOLFOX4 and surgery versus surgery alone for resectable liver metastases from colorectal cancer: a randomised controlled trial, Lancet 371 (2008) 1007–1016.
[2] G.K. Michalopoulos, Liver regeneration, J. Cell Physiol. 213 (2007) 286–300.
[3] Y. Miyaoka, K. Ebato, H. Kato, S. Arakawa, S. Shimizu, A. Miyajima, Hypertrophy and unconventional cell division of hepatocytes underlie liver regeneration, Curr. Biol. 22 (2012) 1166–1175.
[4] G.M. Higgins, R.M. Anderson, Experimental pathology of the liver, Arch. Pathol. 12 (1931) 186–202.
[5] M.A. van den Broek, S.W. Olde Damink, C.H. Dejong, H. Lang, M. Malago, R. Jalan, et al., Liver failure after partial hepatic resection: definition, pathophysiology, risk factors and treatment, Liver Int. 28 (2008) 767–780.
[6] M. Kohjima, T.H. Tsai, B.C. Tackett, S. Thevananther, L. Li, B.H. Chang, et al., Delayed liver regeneration after partial hepatectomy in adipose differentiation related protein-null mice, J. Hepatol. 59 (2013) 1246–1254.
[7] I. Uriarte, M.G. Fernandez-Barrena, M.J. Monte, M.U. Latasa, H.C. Chang, S. Carotti, et al., Identification of fibroblast growth factor 15 as a novel mediator of liver regeneration and its application in the prevention of post-resection liver failure in mice, Gut 62 (2013) 899–910.
[8] D. Cirera-Salinas, M. Pauta, R.M. Allen, A.G. Salerno, C.M. Ramirez, A. Chamorro-Jorganes, et al., Mir-33 regulates cell proliferation and cell cycle progression, Cell Cycle 11 (2012) 922–933.
[9] T.T. Hui, T. Mizuguchi, N. Sugiyama, I. Avital, J. Rozga, A.A. Demetriou, Immediate early genes and p21 regulation in liver of rats with acute hepatic failure, Am. J. Surg. 183 (2002) 457–463.
[10] R. Sun, O. Park, N. Horiguchi, S. Kulkarni, W.I. Jeong, H.Y. Sun, et al., STAT1 contributes to dsRNA inhibition of liver regeneration after partial hepatectomy in mice, Hepatology 44 (2006) 955–966.
[11] V. Witko-Sarsat, M. Friedlander, C. Capeillere-Blandin, T. Nguyen-Khoa, A.T. Nguyen, J. Zingraff, et al., Advanced oxidation protein products as a novel marker of oxidative stress in uremia, Kidney Int. 49 (1996) 1304–1313.
[12] J. Cai, T. Han, C. Nie, X. Jia, Y. Liu, Z. Zhu, et al., Biomarkers of oxidation stress, inflammation, necrosis and apoptosis are associated with hepatitis B-related acute-on-chronic liver failure, Clin. Res. Hepatol. Gastroenterol. 40 (2015) 41–50.
[13] H. Luo, Y. Yang, F. Huang, F. Li, Q. Jiang, K. Shi, et al., Selenite induces apoptosis in colorectal cancer cells via AKT-mediated inhibition of beta-catenin survival axis, Cancer Lett. 315 (2012) 78–85.
[14] W. Cao, F.F. Hou, J. Nie, AOPPs and the progression of kidney disease, Kidney Int. Suppl. 4 (2014) 102–106.
[15] T.J. Guzik, W. Chen, M.C. Gongora, B. Guzik, H.E. Lob, D. Mangalat, et al., Calcium-dependent NOX5 nicotinamide adenine dinucleotide phosphate oxidase contributes to vascular oxidative stress in human coronary artery disease, J. Am. Coll. Cardiol. 52 (2008) 1803–1809.
[16] T. Kahles, R.P. Brandes, Which NADPH oxidase isoform is relevant for ischemic stroke? The case for nox 2, Antioxid. Redox Signal. 18 (2013) 1400–1417.
[17] S.W. Caito, M. Aschner, Mitochondrial redox dysfunction and environmental exposures, Antioxid. Redox Signal. 23 (2015) 578–595.
[18] Xiaoping Xu, Shibo Sun, Fang Xie, Juanjuan Ma, Jing Tang, Shuying He, et al., Advanced oxidation protein products induce epithelial-mesenchymal transition of intestinal epithelial cells via a PKC δ-mediated, redox-dependent signaling pathway, Antioxid. Redox Signal. 27 (2016) 37–56.
[19] N. D'Onofrio, L. Servillo, A. Giovane, R. Casale, M. Vitiello, R. Marfella, et al., Ergothioneine oxidation in the protection against high-glucose induced endothelial senescence: involvement of SIRT1 and SIRT6, Free Radic. Biol. Med. 96 (2016) 211–222.
[20] J. Kim, P.K. Wong, Loss of ATM impairs proliferation of neural stem cells through oxidative stress-mediated p38 MAPK signaling, Stem Cells 27 (2009) 1987–1998.
[21] A.E. Vendrov, K.C. Vendrov, A. Smith, J. Yuan, A. Sumida, J. Robidoux, et al., NOX4 NADPH oxidase-dependent mitochondrial oxidative stress in aging-associated cardiovascular disease, Antioxid. Redox Signal. 23 (2015) 1389–1409.
[22] F. Xie, S. Sun, A. Xu, S. Zheng, M. Xue, P. Wu, et al., Advanced oxidation protein products induce intestine epithelial cell death through a redox-dependent, c-jun N-terminal kinase and poly (ADP-ribose) polymerase-1-mediated pathway, Cell Death Dis. 5 (2014) e1006.
[23] P.M. Chen, C.H. Lin, N.T. Li, Y.M. Wu, M.T. Lin, S.C. Hung, et al., c-Maf regulates pluripotency genes, proliferation/self-renewal, and lineage commitment in ROS-mediated senescence of human mesenchymal stem cells, Oncotarget 6 (2015) 35404–35418.
[24] Q. Wang, L. Xue, X. Zhang, S. Bu, X. Zhu, D. Lai, Autophagy protects ovarian cancer-associated fibroblasts against oxidative stress, Cell Cycle 15 (2016) 1376–1385.
[25] S. Tang, Y. Hou, H. Zhang, G. Tu, L. Yang, Y. Sun, et al., Oxidized ATM promotes abnormal proliferation of breast CAFs through maintaining intracellular redox homeostasis and activating the PI3K-AKT, MEK-ERK, and Wnt-beta-catenin signaling pathways, Cell Cycle 14 (2015) 1908–1924.
[26] G.Z. Tao, N. Lehwald, K.Y. Jang, J. Baek, B. Xu, M.B. Omary, et al., Wnt/beta-catenin signaling protects mouse liver against oxidative stress-induced apoptosis through the inhibition of forkhead transcription factor FoxO3, J. Biol. Chem. 288 (2013) 17214–17224.
[27] H. Aberle, A. Bauer, J. Stappert, A. Kispert, R. Kemler, Beta-catenin is a target for the ubiquitin-proteasome pathway, EMBO J. 16 (1997) 3797–3804.
[28] S.P. Monga, P. Pediaditakis, K. Mule, D.B. Stolz, G.K. Michalopoulos, Changes in WNT/beta-catenin pathway during regulated growth in rat liver regeneration, Hepatology 33 (2001) 1098–1109.
[29] A. Gougelet, C. Sartor, L. Bachelot, C. Godard, C. Marchiol, G. Renault, et al., Antitumour activity of an inhibitor of miR-34a in liver cancer with beta-catenin-mutations, Gut 65 (2016) 1024–1034.
[30] Y. Ma, X. Lv, J. He, T. Liu, S. Wen, L. Wang, Wnt agonist stimulates liver regeneration after small-for-size liver transplantation in rats, Hepatol. Res. 46 (2016) E154–E164.

[31] J.P. Parody, M.P. Ceballos, A.D. Quiroga, D.E. Frances, C.E. Carnovale, G.B. Pisani, et al., FoxO3a modulation and promotion of apoptosis by interferon-alpha2b in rat preneoplastic liver, Liver Int. 34 (2014) 1566–1577.
[32] F. Girard, U. Strausfeld, A. Fernandez, N.J. Lamb, Cyclin A is required for the onset of DNA replication in mammalian fibroblasts, Cell 67 (1991) 1169–1179.
[33] C. Capeillere-Blandin, V. Gausson, B. Descamps-Latscha, V. Witko-Sarsat, Biochemical and spectrophotometric significance of advanced oxidized protein products, Biochim. Biophys. Acta 2004 (1689) 91–102.
[34] H. Liu, T. Han, J. Tian, Z.Y. Zhu, Y. Liu, Y. Li, et al., Monitoring oxidative stress in acute-on-chronic liver failure by advanced oxidation protein products, Hepatol. Res. 42 (2012) 171–180.
[35] D.P. O'Leary, J.H. Wang, T.G. Cotter, H.P. Redmond, Less stress, more success? Oncological implications of surgery-induced oxidative stress, Gut 62 (2013) 461–470.
[36] T. Yukioka, H. Tanaka, K. Ikegami, S. Shimazaki, Free radicals and surgical stress, Nihon Geka Gakkai Zasshi. 97 (1996) 716–720.
[37] M.J. Amaya, A.G. Oliveira, E.S. Guimaraes, M.C. Casteluber, S.M. Carvalho, L.M. Andrade, et al., The insulin receptor translocates to the nucleus to regulate cell proliferation in liver, Hepatology 59 (2014) 274–283.
[38] M.T. Guerra, E.A. Fonseca, F.M. Melo, V.A. Andrade, C.J. Aguiar, L.M. Andrade, et al., Mitochondrial calcium regulates rat liver regeneration through the modulation of apoptosis, Hepatology 54 (2011) 296–306.
[39] Ruoting Ding, Hui Jiang, Baihui Sun, Xiaoliang Wu, Wei Li, Siyuan Zhu, et al., Advanced oxidation protein products sensitized the transient receptor potential vanilloid 1 via NADPH oxidase 1 and 4 to cause mechanical hyperalgesia, Redox Biol. 10 (2016) 1–11.
[40] S. Elumalai, U. Karunakaran, I.K. Lee, J.S. Moon, K.C. Won, Rac1-NADPH oxidase signaling promotes CD36 activation under glucotoxic conditions in pancreatic beta cells, Redox Biol. 11 (2017) 126–134.
[41] L.L. Zhou, F.F. Hou, G.B. Wang, F. Yang, D. Xie, Y.P. Wang, et al., Accumulation of advanced oxidation protein products induces podocyte apoptosis and deletion through NADPH-dependent mechanisms, Kidney Int. 76 (2009) 1148–1160.
[42] K. Bedard, K.H. Krause, The NOX family of ROS-generating NADPH oxidases: physiology and pathophysiology, Physiol. Rev. 87 (2007) 245–313.
[43] Mochel Nabora Soledad Reyes de, Scott Seronello, Shelley Hsiuying Wang, Chieri Ito, Jasper Xi Zheng, T. Jake Liang, et al., Hepatocyte NAD(P)H oxidases as an endogenous source of reactive oxygen species during hepatitis C virus infection, Hepatology 52 (2010) 47–59.
[44] J. Yang, L.E. Mowry, K.N. Nejak-Bowen, H. Okabe, C.R. Diegel, R.A. Lang, et al., beta-catenin signaling in murine liver zonation and regeneration: a Wnt-Wnt situation, Hepatology 60 (2014) 964–976.
[45] D. Sodhi, A. Micsenyi, W.C. Bowen, D.K. Monga, J.C. Talavera, S.P. Monga, Morpholino oligonucleotide-triggered beta-catenin knockdown compromises normal liver regeneration, J. Hepatol. 43 (2005) 132–141.
[46] K.N. Nejak-Bowen, S.P. Monga, Beta-catenin signaling, liver regeneration and hepatocellular cancer: sorting the good from the bad, Semin Cancer Biol. 21 (2011) 44–58.
[47] T.Y. Yang, G.C. Chang, K.C. Chen, H.W. Hung, K.H. Hsu, G.T. Sheu, et al., Sustained activation of ERK and Cdk2/cyclin-A signaling pathway by pemetrexed leading to S-phase arrest and apoptosis in human non-small cell lung cancer A549 cells, Eur. J. Pharmacol. 663 (2011) 17–26.
[48] Y.G. Li, D.F. Ji, S. Zhong, P.G. Liu, Z.Q. Lv, J.X. Zhu, et al., Polysaccharide from Phellinus linteus induces S-phase arrest in HepG2 cells by decreasing calreticulin expression and activating the P27kip1-cyclin A/D1/E-CDK2 pathway, J. Ethnopharmacol. 150 (2013) 187–195.
[49] H. Chen, X. Zeng, C. Gao, P. Ming, J. Zhang, C. Guo, et al., A new arylbenzofuran derivative functions as an anti-tumour agent by inducing DNA damage and inhibiting PARP activity, Sci. Rep. 5 (2015) 10893.
[50] S. Lim, P. Kaldis, Cdks, cyclins and CKIs: roles beyond cell cycle regulation, Development 140 (2013) 3079–3093.
[51] C.J. Sherr, J.M. Roberts, CDK inhibitors: positive and negative regulators of G1-phase progression, Genes Dev. 13 (1999) 1501–1512.
[52] M. Ohtsubo, A.M. Theodoras, J. Schumacher, J.M. Roberts, M. Pagano, Human cyclin E, a nuclear protein essential for the G1-to-S phase transition, Mol. Cell Biol. 15 (1995) 2612–2624.
[53] R.W. King, P.K. Jackson, M.W. Kirschner, Mitosis in transition, Cell 79 (1994) 563–571.
[54] S. Paternot, B. Colleoni, X. Bisteau, P.P. Roger, The CDK4/CDK6 inhibitor PD0332991 paradoxically stabilizes activated cyclin D3-CDK4/6 complexes, Cell Cycle 13 (2014) 2879–2888.